RSC Advances

ROYAL SOCIETY OF CHEMISTRY

www.rsc.org/advances

Journal Name

RSCPublishing

COMMUNICATION

$MgVPO_4F$ as a one-dimensional Mg-ion conductor for Mg ion battery positive electrode: a first principles calculation

Cite this: DOI: 10.1039/xoxxoooooox

Received ooth January 2012,
Accepted ooth January 2012

DOI: 10.1039/xoxxoooooox

www.rsc.org/

Jiandong Wu, Guohua Gao*, Guangming Wu*, Bo Liu, Huiyu Yang, Xiaowei Zhou, Jichao Wang

$MgVPO_4F$ is proposed as a cathode material for rechargeable Mg ion batteries for the first time. First principles calculations were performed to study the electrochemical properties of $MgVPO_4F$ as a positive electrode material for rechargeable Mg ion batteries. Our theoretical study gives an expectation of good battery performance by $MgVPO_4F$.

Introduction

Despite the successful application of Li ion battery (LIB) in portable electronics in the past decades, the high prices and low energy density of LIB still limit its application in plug-in hybrid electric vehicles and electric vehicles[1, 2]. To increase the energy density, new battery systems such as Li-S and Li-air batteries have been extensively studied. Mg ion battery (MIB) [3-7] is another candidate for its safety of handling, higher volumetric energy density, high negative reduction potential and low cost. However, only a few materials can be used for positive electrode of MIB，including Chevrel phase $M_xMo_6T_8$(M=metal, T=S, Se)[8-11], TiS_2 nanotubes[12], graphene-like MoS_2[13], $Mg_xCo_3O_4$[14], α-MnO_2[15] and mesoporous $Mg_{1.03}Mn_{0.97}SiO_4$[16]. The development of MIB is mainly limited by the low Mg ions mobility in positive electrode. It shows a high activation barrier for Mg ion diffusion in many bulk electrode materials, largely due to the divalent nature of Mg ions, which have strong interaction with anions and cations in positive electrode materials[17, 18].

First principles calculations were used to design and develop new electrode materials for MIB. Ling et al.[19] investigated the electrochemical properties of $TMSiO_4$(TM=Fe, Mn, Co, Ni) as cathode for MIB, and the redox reaction mechanism in the magnesiation of $TMSiO_4$ were studied. According to the results from Yang et al.[20] the Mg^{2+} diffusion barrier on the zigzag MoS_2 nanorribbon was found to be 0.48 eV, which is much lower than that of bulk MoS_2 material. In particular, Ling et al.[21] found that the diffusion activation energy of Mg^{2+} in $CaFe_2O_4$-type $MgMn_2O_4$ is 0.4eV, which is comparable with that of Li^+ in typical LIB cathode materials.

As Li_2VPO_4F[22] shows a capacity of 312 $mAhg^{-1}$ and the activation energy for Li diffusion in VPO_4F is only 0.33 eV[23]. Hence, we dare to propose $MgVPO_4F$ as a new candidate positive electrode material for MIB. With the introduction of F anions, we expect a relative weak interaction between Mg ion and anions and better ionic conductivity. To the best of our knowledge, this is the first time $MgVPO_4F$ has been proposed as a positive electrode material for MIB.

In this paper, based on first principles calculations, the crystal structures of Mg_xVPO_4F(x=0, 0.5 and 1) were obtained, and the OCV of $MgVPO_4F$ as a positive electrode for MIB were calculated. Then, the electronic structures and Bader charge for Mg_xVPO_4F(x=0, 0.5 and 1) were studied to reveal the redox reaction mechanism as Mg intercalation into VPO_4F. Finally, the diffusion activation energy for Mg ions along [100], [010], [101] and [111] direction of $Mg_{1-x}VPO_4F$ were calculated to study the Mg ion conductivity of $MgVPO_4F$.

Methodology

The present calculations were performed using the Vienna ab initio simulation package(VASP)[24] with projector augmented wave pseudo potentials [25, 26] (PAW) approach. The exchange and correlation energy functional were treated by the Perdew–Burke–Ernzerhof variant of the generalized gradient approximation(GGA)[27] and GGA+U[28] extension to it, and a U_{eff}=3.1 eV was adapted for V, similar value has been used for $LiVPO_4F$[23]. The energy cutoff for the plane wave basis set was set to be 500eV, and the total energy was converged to 10^{-5} eV. A k-points sampling of $8\times8\times6$ was used to ensure the energies were converged within 5 meV per formula unit. In addition, the single point energies were calculated with different magnetic alignments including FM (ferromagnetic) and AFM (antiferromagnetic). The climbing-image nudged elastic band (Cl-NEB)[29] method implemented in VASP was used to f investigate the Mg ion diffusion property in $Mg_{1-x}VPO_4F$. A super cell containing $2\times2\times2$ unit cells was used to ensure that no magnesium ion vacancy was within 8 Å from its periodic image. The volume was frozen and only the k-point at Γ(center of Brillouin zone) was used. Ions in the super cell were relaxed with Quick-Min(QM) method as implemented in the VASP Transition State Tools. The NEB calculations were deemed to be converged when the force on each image was less than 0.03 $eVÅ^{-1}$.

Results and discussion

The structure of $LiVPO_4F$[22] was used as the template for $MgVPO_4F$, after fully relaxation, Mg atoms were removed to obtain the structures of $Mg_{0.5}VPO_4F$ and VPO_4F. The calculations predict FM ground states for VPO_4F and $Mg_{0.5}VPO_4F$, and AFM ground states for $MgVPO_4F$. As shown in Fig.1, $MgVPO_4F$ is composed by corner-shared VO_4F_2 octahedral chains connected by PO_4 tetrahedrons, with Mg ions located in the framework. $MgVPO_4F$ crystallize in the triclinic space group P-1 with two vanadium atoms occupy at 1a (0, 0, 0) and 1b (0, 0, 1/2) site respectively, and with Mg, O, P and F atoms occupy at 2i sites. After remove half Mg atoms from $MgVPO_4F$, the structure of $Mg_{0.5}VPO_4F$ crystallize in the triclinic space group P-1, the decrease of structure symmetry is mainly caused by the strong distortion of VO_4F_2 octahedron. VPO_4F crystallize in the monoclinic space group C2/c, with V atoms occupy at 4b sites, and F and P atoms occupy at 4e sites, and O atoms occupy at 8f sites. The lattice parameters of Mg_xVPO_4F(x=0, 0.5 and 1) are listed in Table1. The parameters of primitive cell of VPO_4F were obtained based on the data in Ref[30], all the lattice parameters of VPO_4F are a little overestimated, which is a reasonable error for the use of GGA+U[31, 32]. Up on half magnesiation, the volume of VPO_4F is predicted to increase by 8.0%. However, further magnesiation from $Mg_{0.5}VPO_4F$ to $MgVPO_4F$ also lead to a volume expansion about 8.2%, which is similar with the volume expansion from $LiVPO_4F$ to Li_2VPO_4F[30]. This indicated that full magnesiation of VPO_4F might cause structure instability, which is harmful to its cycle performance. Hence, charge/discharge $Mg_{0.5}VPO_4F$ with half Mg might be a reasonable option.

Table 1 Structure parameters of Mg_xVPO_4F(x=0, 0.5 and 1)

	a/Å	*b*/Å	*c*/Å	α/°	β/°	γ/°	V/Å^3
VPO_4F	**5.175**	**5.175**	**7.501**	**110.754**	**110.754**	**91.655**	**172.90**
Exp.[30]	**5.041**	**5.041**	**7.116**	**109.523**	**109.523**	**89.567**	**159.50**
$Mg_{0.5}VPO_4F$	**5.289**	**5.405**	**7.487**	**108.911**	**107.866**	**97.139**	**186.688**
$MgVPO_4F$	**5.310**	**5.687**	**7.557**	**108.411**	**106.940**	**96.315**	**201.920**

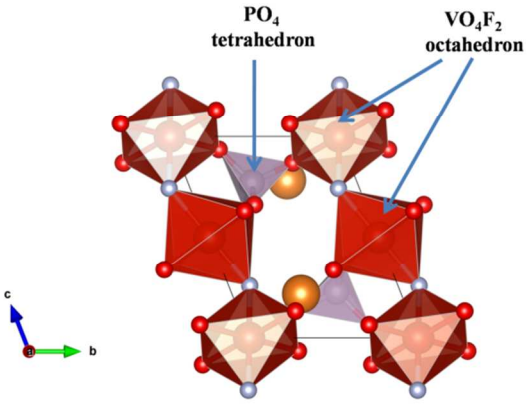

Fig.1 Crystal structure of $MgVPO_4F$: the red octahedra represent VO_4F_2, light magenta tetrahedron represent PO_4, red spheres represent O, dark gray spheres represent F and orange spheres represent Mg.

The average OCV was obtained by calculating the difference of chemical potential between positive electrode (VPO_4F) and negative electrode (Mg)[19]. $MgVPO_4F$ shows two discharge plateaus at 2.6 V and 1.5 V corresponding to the redox couples of V^{4+}/V^{3+} and V^{3+}/V^{2+}. Each electrochemical reaction shows a theoretical capacity about 156mAhg^{-1}. Hence, if fully discharged, VPO_4F might show a high theoretical specific capacity about 312 mAhg^{-1}.

In order to analyze the redox reaction mechanism as Mg intercalation into VPO_4F, the density of states for VPO_4F, $Mg_{0.5}VPO_4F$ and $MgVPO_4F$ were studied in detail. Fig.2 shows the total density of states (TDOS) for Mg_xVPO_4F and partial density of states (PDOS) for V-3*d*, O-2*p* and F-2*p* orbital, and the Fermi level is set at zero energy. In all three compounds, the valance bands of V-3*d* between -8 eV and -1 eV are hybridized with O-2*p* and F-2*p* bands. The *p*-*d* hybridization of V-O and V-F at low energy range is going to make a contribution to the stability of crystal structure. In VPO_4F, the PDOS of V-3*d* for V_1 and V_2 are nearly the same, indicating they have the same electronic structure. When VPO_4F was magnesiated into $Mg_{0.5}VPO_4F$, the electrons provided by Mg are mainly localized at V-3*d* orbital at the top valence band, and both V^{4+} are reduced into V^{3+}. While $Mg_{0.5}VPO_4F$ was magnesiated into $MgVPO_4F$, the magnetic alignment changed from FM to AFM, and V^{3+} were reduced into V^{2+}. The redox reaction mechanism is similar with the magnesiation of $MnSiO_4$[19].

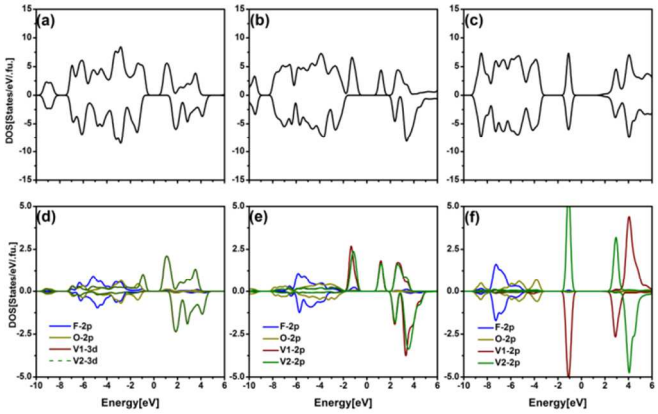

Fig.2 The total density of states (TDOS) for Mg_xVPO_4F: (a) VPO_4F, (b) $Mg_{0.5}VPO_4F$ and (c) $MgVPO_4F$, and the Partial density of states (PDOS) of V-3*d*, O-2*p* and F-2*p* for (d) VPO_4F, (e) $Mg_{0.5}VPO_4F$, (f) $MgVPO_4F$, and the Fermi level is set at zero energy.

To analyze the charge transfer between Mg and the positive electrode host quantitatively, the average Bader[33-35] charge around each nucleus were calculated. As shown in Table 2, the Bader charges on Mg in $Mg_{0.5}VPO_4F$ and $MgVPO_4F$ are +1.70 *e* and +1.69 *e*, indicating the ionization of Mg. For VPO_4F, $Mg_{0.5}VPO_4F$ and

$MgVPO_4F$, the charge of V are +2.30 *e*, +2.03 *e* and 1.58 *e*, respectively, suggesting its strong covalent interactions with O and F atoms. The Bader charge of V_1 and V_2 in $Mg_{0.5}VPO_4F$ and $MgVPO_4F$ are the same (+2.03 *e* and 1.58 *e*), indicating that the insertion of one Mg reduced two VO_4F_2 units instead of reducing only one VO_4F_2 unit.

Table 2 Average Bader charge (*e*) of Mg, V, O, P and F for Mg_xVPO_4F

	Mg	F	O	P	V_1	V_2
VPO_4F		-0.67	-1.33	+3.68	+2.30	+2.30
$Mg_{0.5}VPO_4F$	+1.70	-0.75	-1.45	+3.68	+2.03	+2.03
$MgVPO_4F$	+1.69	-0.82	-1.52	+3.66	+1.57	+1.58

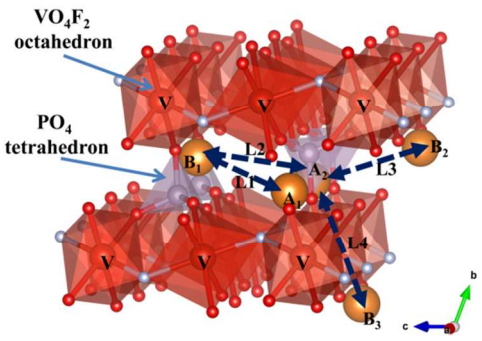

Fig.3 The diffusion pathways for Mg diffusion along [100] , [010] , [101] and [111] directions. The red octahedra represent VO_4F_2, light magenta tetrahedron represent PO_4, red spheres represent O, dark gray spheres represent F and orange spheres represent Mg.

In order to investigate Mg ion conductivity in $Mg_{1-x}VPO_4F$, the Cl-NEB method implemented in VASP was performed. Fig.3 shows the diffusion paths for Mg diffusion along [100], [010], [101] and [111] directions. All the Mg ion migration paths are a combination of two diagonal jumps, and these diagonal jumps form continuous diffusion paths. Jumps involved in each diffusion direction and the calculated activation energies for the diffusion paths in $Mg_{1-x}VPO_4F$ are listed in Table 3.

The energy barrier for Mg ion diffusion along [111] direction is 0.704 eV, which is much lower than that of bulk V_2O_5[36](1.40 eV) and MoS_2[20](2.61 eV). The activation energy for hops in other direction are at least 700meV higher than the activation energy along [111], making $Mg_{1-x}VPO_4F$ a 1D diffuser for Mg ion battery. This appeared to be similar with the paths for lithium diffusion in VPO_4F[23].

A rough diffusion coefficient can be estimate as

$$D = a^2 \nu e^{(-E_A/kT)}$$

Where *a* is the distant of a diffusion jump, ν is the attempt frequency and E_A is the activation energy, and *kT* is Boltzmann's constant times the temperature. In this calculation, a typical value of 10^{13} s^{-1} was used for *v*, and the temperature was assumed to be 300*K*. An estimated diffusion coefficient using the lowest activation energy is in the order of 10^{-14} cm^2/s. Therefore, we can expect better Mg ion conductivity for $MgVPO_4F$. Here, we stress that the estimated diffusion coefficient requires unblocked channel.

Table 3 Activation Energies for paths in $Mg_{1-x}VPO_4F$

Diffusion direction	Jumps involved	Activation energy(eV)
[100]	L1+L2	1.597
[010]	L3+L4	1.483
[101]	L2+L3	1.483
[111]	L2+L4	0.704

Conclusions

Based on First principles calculations, $MgVPO_4F$ is proposed as a new candidate positive electrode material for MIB. Two intercalation plateaus at 2.6 and 1.5 V corresponding to the redox couples of V^{4+}/V^{3+} and V^{3+}/V^{2+} were predicted, and each electrochemical reaction shows a theoretical specific capacity about 156mAhg^{-1}. In addition, the redox reaction mechanism was revealed in the process of Mg intercalation into VPO_4F. V^{4+} was reduced into V^{3+} when $Mg_{0.5}VPO_4F$ formed, and further reduction of V^{3+} into V^{2+} took place as $MgVPO_4F$ formed. The Bader Charge Analysis indicating that the insertion of one Mg reduced two VO_4F_2 units instead of reducing only one VO_4F_2 unit. The lowest energy barrier for Mg-ion migrates in $Mg_{1-x}VPO_4F$ is along [111], and the corresponding activation energy is in the order of 0.704 eV, which is much lower than that of bulk V_2O_5 and MoS_2. The present results give expectation of good battery performance by $MgVPO_4F$. We believe this work will facilitate the future research of MIB with high performance.

Acknowledgements

The authors gratefully acknowledge the financial support by National Natural Science Foundation of China (grant numbers 51272179, 51072137, 51102183), Doctor Subject Fund of Education Ministry of China (grant no. 20100072110054), Shanghai Committee of Science and Technology(11nm0501300, 13JC1408700), National high-tech R-D program of china(863 program) (grant no.2013AA031801)

Notes and references

*Email: gao@tongji.edu.cn;wugm@tongji.edu.cn;
Shanghai Key Laboratory of Special Artificial Microstructure, Tongji University, Shanghai, P. R. China.

1. J. M. Tarascon, *Philosophical Transactions of the Royal Society a-Mathematical Physical and Engineering Sciences*, 2010, 368, 3227-3241.
2. J. M. Tarascon and M. Armand, *Nature*, 2001, 414, 359-367.
3. M. Morita, N. Yoshimoto, S. Yakushiji and M. Ishikawa, *Electrochemical and Solid State Letters*, 2001, 4, A177-A179.
4. D. Aurbach, Z. Lu, A. Schechter, Y. Gofer, H. Gizbar, R. Turgeman, Y. Cohen, M. Moshkovich and E. Levi, *Nature*, 2000, 407, 724-727.
5. D. Aurbach, G. S. Suresh, E. Levi, A. Mitelman, O. Mizrahi, O. Chusid and M. Brunelli, *Adv. Mater.*, 2007, 19, 4260-+.
6. E. Levi, Y. Gofer and D. Aurbach, *Chem. Mater.*, 2010, 22, 860-868.
7. P. Novak, R. Imhof and O. Haas, *Electrochim. Acta*, 1999, 45, 351-367.
8. K. R. Kganyago, P. E. Ngoepe and C. R. A. Catlow, *Phys. Rev. B: Condens. Matter*, 2003, 67.
9. E. Levi, E. Lancry, A. Mitelman, D. Aurbach, G. Ceder, D. Morgan and O. Isnard, *Chem. Mater.*, 2006, 18, 5492-5503.

10. E. Levi, E. Lancry, A. Mitelman, D. Aurbach, O. Isnard and D. Djurado, *Chem. Mater.*, 2006, 18, 3705-3714.
11. E. Levi, A. Mitelman, O. Isnard, M. Brunelli and D. Aurbach, *Inorg. Chem.*, 2008, 47, 1975-1983.
12. Z. L. Tao, L. N. Xu, X. L. Gou, J. Chen and H. T. Yuan, *Chem. Commun.*, 2004, 2080-2081.
13. Y. L. Liang, R. J. Feng, S. Q. Yang, H. Ma, J. Liang and J. Chen, *Adv. Mater.*, 2011, 23, 640-+.
14. T. E. Sutto and T. T. Duncan, *Electrochim. Acta*, 2012, 80, 413-417.
15. R. G. Zhang, X. Q. Yu, K. W. Nam, C. Ling, T. S. Arthur, W. Song, A. M. Knapp, S. N. Ehrlich, X. Q. Yang and M. Matsui, *Electrochem. Commun.*, 2012, 23, 110-113.
16. Y. N. NuLi, Y. P. Zheng, F. Wang, J. Yang, A. I. Minett, J. L. Wang and J. Chen, *Electrochem. Commun.*, 2011, 13, 1143-1146.
17. E. Levi, M. D. Levi, O. Chasid and D. Aurbach, *J. Electroceram.*, 2009, 22, 13-19.
18. G. G. Amatucci, F. Badway, A. Singhal, B. Beaudoin, G. Skandan, T. Bowmer, I. Plitza, N. Pereira, T. Chapman and R. Jaworski, *J. Electrochem. Soc.*, 2001, 148, A940-A950.
19. C. Ling, D. Banerjee, W. Song, M. J. Zhang and M. Matsui, *J. Mater. Chem.*, 2012, 22, 13517-13523.
20. S. Q. Yang, D. X. Li, T. R. Zhang, Z. L. Tao and J. Chen, *Journal of Physical Chemistry C*, 2012, 116, 1307-1312.
21. C. Ling and F. Mizuno, *Chem. Mater.*, 2013, 25, 3062-3071.
22. J. M. A. Mba, C. Masquelier, E. Suard and L. Croguennec, *Chem. Mater.*, 2012, 24, 1223-1234.
23. T. Mueller, G. Hautier, A. Jain and G. Ceder, *Chem. Mater.*, 2011, 23, 3854-3862.
24. G. Kresse and J. Furthmuller, *Comp. Mater. Sci.*, 1996, 6, 15-50.
25. P. E. Blochl, *Phys. Rev. B: Condens. Matter*, 1994, 50, 17953-17979.
26. G. Kresse and D. Joubert, *Phys. Rev. B: Condens. Matter*, 1999, 59, 1758-1775.
27. J. P. Perdew, K. Burke and M. Ernzerhof, *Phys. Rev. Lett.*, 1996, 77, 3865-3868.
28. S. L. Dudarev, G. A. Botton, S. Y. Savrasov, C. J. Humphreys and A. P. Sutton, *Phys. Rev. B: Condens. Matter*, 1998, 57, 1505-1509.
29. G. Henkelman, B. P. Uberuaga and H. Jonsson, *J. Chem. Phys.*, 2000, 113, 9901-9904.
30. B. L. Ellis, T. N. Ramesh, L. J. M. Davis, G. R. Goward and L. F. Nazar, *Chem. Mater.*, 2011, 23, 5138-5148.
31. Y. Koyama, I. Tanaka, M. Nagao and R. Kanno, *J. Power Sources*, 2009, 189, 798-801.
32. M. Nakayama, M. Kanekoa and M. Wakihara, *PCCP*, 2012, 14, 13963-13970.
33. G. Henkelman, A. Arnaldsson and H. Jonsson, *Comp. Mater. Sci.*, 2006, 36, 354-360.
34. E. Sanville, S. D. Kenny, R. Smith and G. Henkelman, *J. Comput. Chem.*, 2007, 28, 899-908.
35. W. Tang, E. Sanville and G. Henkelman, *Journal of Physics-Condensed Matter*, 2009, 21.
36. Z. G. Wang, Q. L. Su and H. Q. Deng, *PCCP*, 2013, 15, 8705-8709.

